

# Study on Analysis of Torque-Slip Characteristics of Axial Gap Induction Motor

R. Sakai, Y. Yoshida\*, and K. Tajima

Department of Cooperative Major in Life Cycle Design Engineering, Akita Univ., 1-1, Tegata Gakuen-machi, Akita 010-5802, Japan

\*Department of Electrical and Electronic Engineering, Akita Univ., 1-1, Tegata Gakuen-machi, Akita 010-5802, Japan

In this paper, we propose a high-torque-density axial gap induction motor with toroidal winding. It generates a large torque density because it has a high space factor for reducing motor volume and a wide gap face for improving motor torque. First, the structure and design criteria of the proposed motor are described. Next, the torque-slip characteristic of the proposed motor is compared with the induction motor of the conventional structure, which has the same size. Finally, we show an optimized torque density for the proposed motor. The validity of the proposed motor is demonstrated in a three dimensional-finite element analysis (3D-FEA).

**Key words:** induction motor, toroidal winding, axial gap induction motor, finite element analysis

## 1. Introduction

Recently, interest in environmental problems caused by global warming has been increasing every year. Therefore, the demand for using electric vehicles (EVs) and hybrid electric vehicles (HEVs) has been increasing since they emit less carbon dioxide than conventional vehicles. Permanent magnet synchronous motors (PMSMs) are widely used as motors for EVs and HEVs because of their high torque and high efficiency performance. However, due to the rising prices of the rare-earth materials used for PMSMs, rare-earth free motors with high performance must be developed<sup>1)2)</sup>. In comparison, induction motors (IMs) have several advantages because of their simple structure with no permanent magnet; they can rotate at high speed, have a robust structure, and are not affected by soaring rare-earth prices. However, it is difficult for IMs to generate high torque because of the magnet-free structure. Because the excitation current of IMs is applied to the primary winding, there is a risk of heat generation and magnetic saturation. Thus, the torque density and efficiency of IMs must be improved<sup>3)</sup>.

Recently, several techniques effective at increasing the torque density of motors have been reported. Toroidal winding can improve the space factor and reduce the coil end length better compared with distributed winding, thus increasing torque density<sup>4)</sup>.

With an axial gap motor, it is easier to increase the gap area compared with the conventional motor; thus, is suitable for improving torque<sup>5)</sup>. Axial gap induction motors (AGIMs) have an advantage in that the axial length can be shortened compared with conventional radial gap induction motors (RGIMs). This is because the gap area does not depend on the axial length and the coil end is not in the axial direction<sup>6)7)</sup>. In addition, by applying toroidal winding to AGIMs, the coil end can be reduced compared with the conventional distributed winding structure. Since reducing the coil end

contributes to miniaturizing the stator, a further increase in torque density can be expected.

In this paper, we propose an AGIM that is aimed at improving the output torque characteristic. First, an AGIM is designed with the same dimensions as an RGIM used for comparison with a conventional structure. Second, simulation results of the basic properties of the AGIM are compared with those of the RGIM. It was clarified that the proposed AGIM has a doubled output torque density compared with the conventional RGIM.

## 2. Design Method

### 2.1 RGIM to be compared

Figure 1 shows the RGIM to be compared. This RGIM exhibits the dimensions of an actual machine. Motor specifications are shown in Table 1. The motor diameter was 100 mm, the core thickness was 30 mm, the motor thickness including the coil end was 58 mm, and the gap width was 0.35 mm. The winding method was lap winding. Four poles were formed with 24 slots. The proposed AGIM was designed on the bases of Table 1.

### 2.2 Stator structure of AGIM

Figure 2 shows the coil arrangement of the toroidal winding of the axial gap motor. The coils are wound concentrically around the slot and yoke. Toroidal winding can generate the same magnetomotive force as lap winding without coils overlapping with each other. In this paper, we set the space factor of toroidal winding to 40%; if interference does not exist on the inner diameter side, the space factor can be increased further. The proposed AGIM has a single stator and double rotor, which can increase the air-gap area to generate a larger torque compared with that of the conventional RGIM. Figure 3 shows the magnetomotive force distribution of the RGIM and AGIM. Toroidal winding generates magnetomotive force to both sides of the stator plane.

Figure 4 shows the stator structure of the AGIM, which has U-phase toroidal winding. The teeth are placed on two planes, from which magnetic flux flows to the rotor. The motor diameter, gap length, number of poles, number of slots, number of turns, and open width of the slots of the AGIM were set to the same dimensions as those of the RGIM. The cross-sectional area of the slot the AGIM was smaller than that of the RGIM since the proposed AGIM can increase the slot occupancy with toroidal winding.

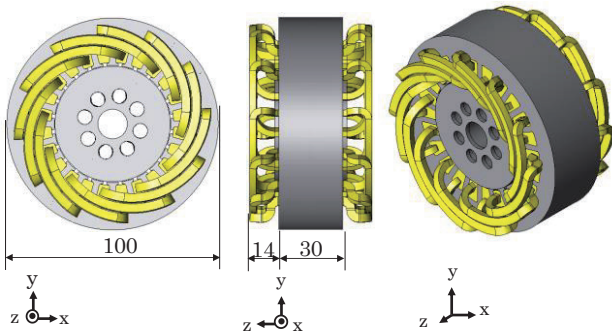


Fig. 1 RGIM to be compared.

Table 1 Specifications of RGIM.

Stator diameter	100 mm
Core thickness	30 mm
Motor axial length	58 mm
Air gap length	0.35 mm
Number of poles	4
Number of slots (stator/rotor)	24/34
Winding method	distributed winding (lap winding)
Number of windings	40
Wire diameter	0.5 mm
Space factor	11%
Secondary conductor cross-sectional area	9.62 mm <sup>2</sup>

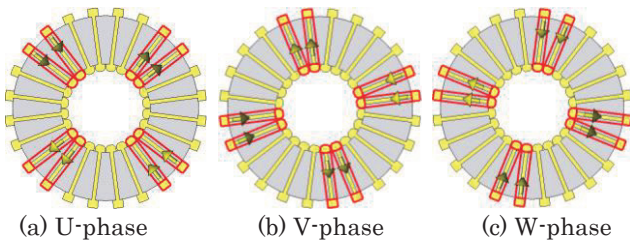


Fig. 2 Coil arrangement of toroidal winding with axial gap motor.

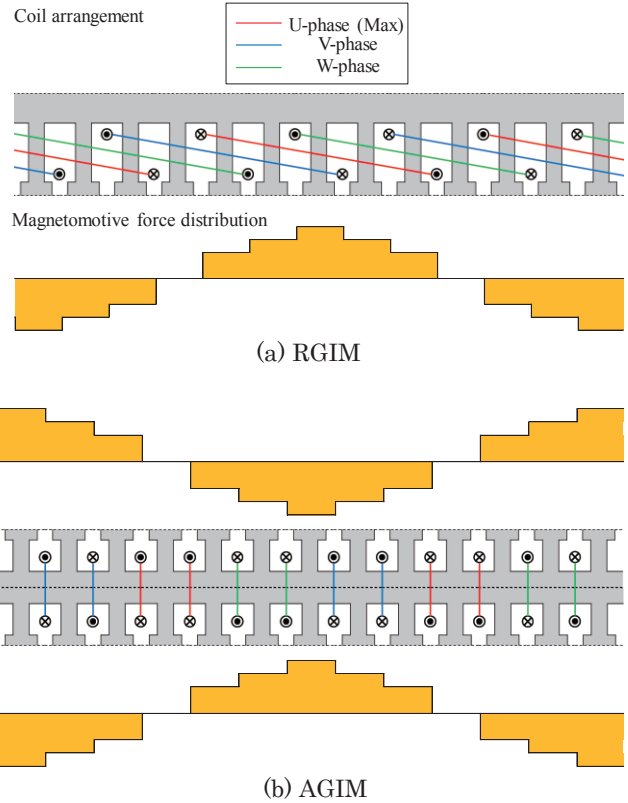


Fig. 3 Coil arrangement and magnetomotive force distribution of RGIM and AGIM.

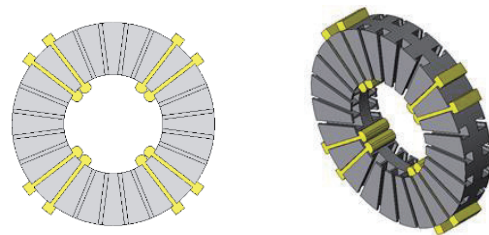


Fig. 4 Stator of AGIM with U-phase toroidal windings.

### 2.3 Rotor structure of AGIM

Figure 5 shows one side of the rotor structure of the AGIM. The cross-sectional area of the rotor bar has the same area as that of the RGIM. The inner and outer diameters of the rotor core were set to the same dimensions as those of the stator core. The opening width of the slot is equal to the rotor of the RGIM. Another rotor of similar shape was prepared to construct a double rotor structure.

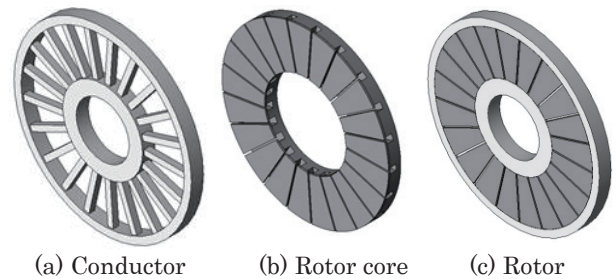


Fig. 5 Rotor structure of AGIM.

## 2.4 Yoke thickness design

The design of the yoke thickness is important for avoiding magnetic saturation. In a general design method, an optimum thickness is set for an assumed magnetic flux amount<sup>8)</sup>. However, in this paper, the cross-sectional area of slots and the number of slots were designed to be equal to those of the RGIM, so the yoke thickness was limited. Since magnetic flux forms a circle via mutual yokes, the thicknesses of the stator and rotor yokes are required to be equal. However, magnetic flux leakage is generated in the rotor yoke with a single stator-double rotor structure. Therefore, the rotor yoke thickness was designed to be 5% thicker than the stator yoke thickness. In this paper, we used two AGIMs. One had a motor thickness of 30 mm, so we set the yoke thickness to be equal to the RGIM core thickness. The second had a motor thickness of 58 mm, which equaled the thickness of the RGIM thickness including the coil end. This was done by increasing the yoke thickness of the 30 mm AGIM by 28 mm. Increasing the thickness of the stator yoke by 14 mm and the two rotor yokes by 7 mm each made this AGIM 28 mm thicker. Figure 6 shows the method of designing the yoke thickness.

Figure 7 shows the designed model, and Table 2 shows the designed motor specifications. Hereinafter AGIM with motor thickness of 30 mm is written AGIM (30 mm), AGIM of 58 mm is AGIM (58 mm).

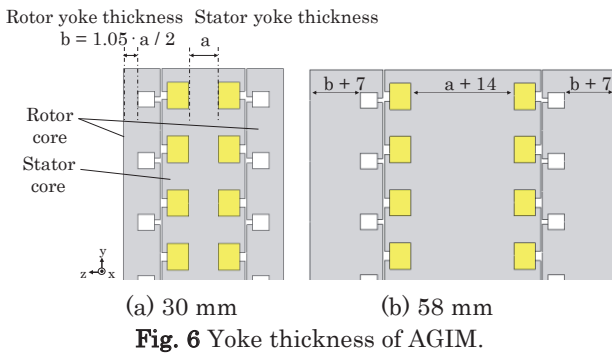


Fig. 6 Yoke thickness of AGIM.

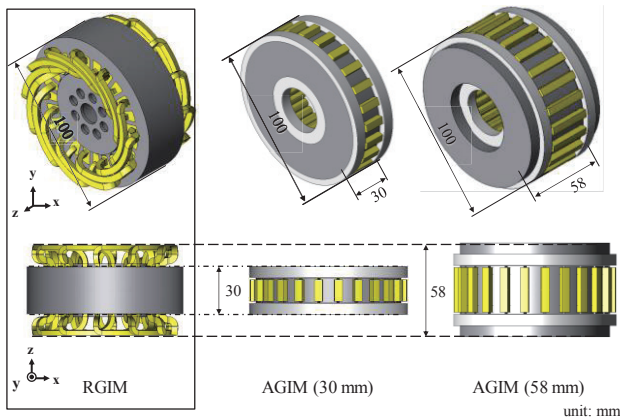


Fig. 7 Overview of designed motor.

## 3. Torque-Slip Characteristic Analysis

In this section, simulation results are described with the simulation model shown in Figure 7. Table 3 shows the simulation conditions. Generally, transient response analysis is used in motor analysis. However, it takes a lot of time to calculate the torque-slip characteristics of an induction motor. In this paper, the magnetic field distribution in the slip state was analyzed by using frequency response analysis with the JMAG-Designer Ver.16.0 software for three-dimensional finite element analysis (3D-FEA). The frequency range was determined to be 50 Hz at a maximum from the operating frequency of an actual machine. The current amplitude applied to the motors was 4 A. Table 4 shows data on the materials of the motors, and Figure 8 shows the mesh of the simulation model. Although various issues arise when manufacturing an actual machine, non-oriented electromagnetic steel were used for the core of the AGIMs without considering the stacking direction. Therefore, comparison was made between the AGIMs and RGIM by using the same material.

Table 2 Specifications of designed AGIM.

Stator diameter	100 mm
Motor axial length	30 mm
Air gap length	0.35 mm
Yoke thickness of 30 mm (stator/rotor)	5.6/2.65 mm
Yoke thickness of 58 mm (stator/rotor)	19.6/9.65 mm
Number of poles	4
Number of slots (stator/rotor)	24/34
Winding method	Toroidal winding
Number of windings	40 turns
Wire diameter	0.5 mm

Table 3 Simulation condition.

Simulation mode	Frequency response analysis
Step	31
Frequency range	0.5 ~ 50 Hz
Current amplitude	4 A

Table 4 Simulation model material.

Stator core	50A230
Rotor core	50A230
Coil	Cu
Rotor conductor	Al
Shaft	Air

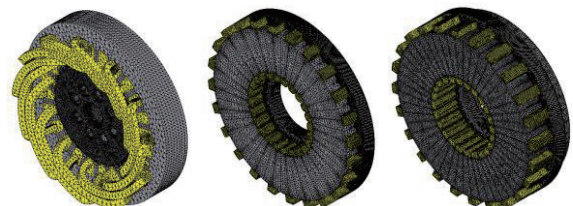


Fig. 8 Mesh of analysis model.

Figure 9 shows the torque-slip characteristics of the three motors, and Table 5 shows a comparison of the maximum torque and torque density. Comparing the characteristics of the AGIMs and RGIM, the maximum torque of AGIM (30 mm) was equivalent to that of the RGIM, and the maximum torque of AGIM (58 mm) was double that of the RGIM. Comparing the characteristics of the two AGIMs, which differed in axial length, the starting torques were equal. The more the slip decreased, the more a torque difference appeared. When the slip was small, the input frequency was low. The magnetic flux density became high because the magnetic flux density flowing in the core was in inverse proportion to the frequency as:

$$B_m = k \frac{E}{f \cdot A} \quad (1)$$

where  $B_m$  is the maximum magnetic flux density,  $k$  is the factor of proportionality,  $E$  is the input voltage,  $f$  is the input frequency, and  $A$  is a cross-sectional area<sup>9)</sup>. Therefore, it is expected that the magnetic saturation will occur in the core of AGIM (30 mm) when the slip is small. Figure 10 shows the magnet flux density distribution of AGIM (30 mm) and AGIM (58 mm) at  $s = 0.05$ . The magnetic saturation in the back yoke of AGIM (30 mm) caused a smaller maximum torque than that of AGIM (58 mm). Therefore, the expected torque is obtained with AGIM (58 mm) without saturation of the magnetic flux density.

Next, a comparison of torque density between the three motors is described. The motor volume  $V$  is calculated from

$$V = \frac{1}{4} \pi \cdot D^2 \cdot h \quad (2)$$

where  $D$  is the motor diameter and  $h$  is the motor thickness. The volume of the RGIM and AGIM (58 mm) were equal, and AGIM (30 mm) was about half that of the RGIM. Since the maximum torque of AGIM (58 mm) was double that of the RGIM and the volume of AGIM (30 mm) was half that of RGIM, the torque densities of both AGIMs were double that of the RGIM.

#### 4. Consideration of Torque density

The torque density of AGIM (30 mm) became larger than that of the AGIM (58 mm). The reason for this is that AGIM (30 mm) had a volume that was smaller than that of the AGIM (58 mm) by 48%. The variation in torque was computed by changing the motor axis length from 30 to 58 mm in order to find the condition where the torque density was maximum. Figure 11 shows how the yoke thickness was set. When the stator yoke thickness “a” was increased by 2 mm, the rotor yoke thickness “b” was increased by 1 mm; the total motor thickness was increased by 4 mm. Thus, the motor thickness was varied by 4 mm from 30 to 58 mm. Figure 12 shows the torque-slip characteristics at each motor thickness. As the motor thickness increased, the

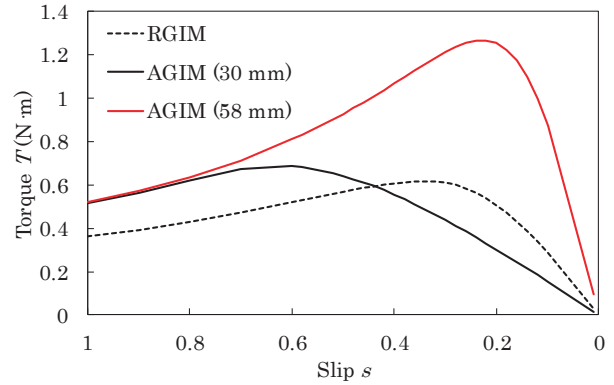


Fig. 9 Torque-slip characteristic.

Table 5 Comparison of max torque and torque density.

	RGIM	AGIM (30 mm)	AGIM (58 mm)
Max torque (N·m)	0.617	0.686	1.266
Volume (L)	0.456	0.236	0.456
Torque density (N·m/L)	1.353	2.907	2.776
Maximum torque ratio	1	1.112	2.052
Torque density ratio	1	2.149	2.052

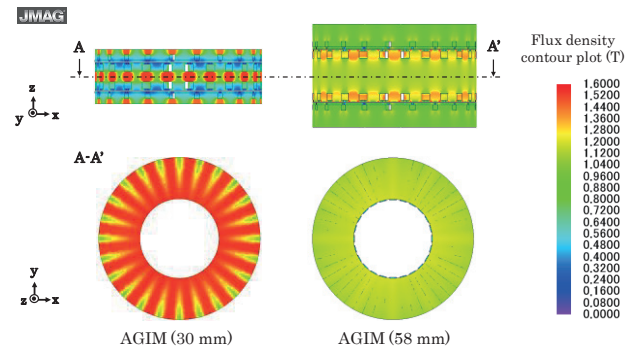
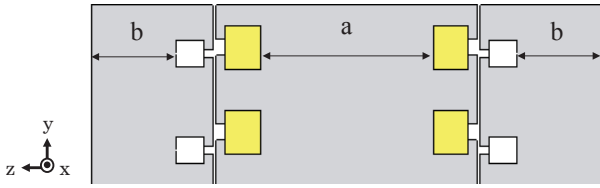
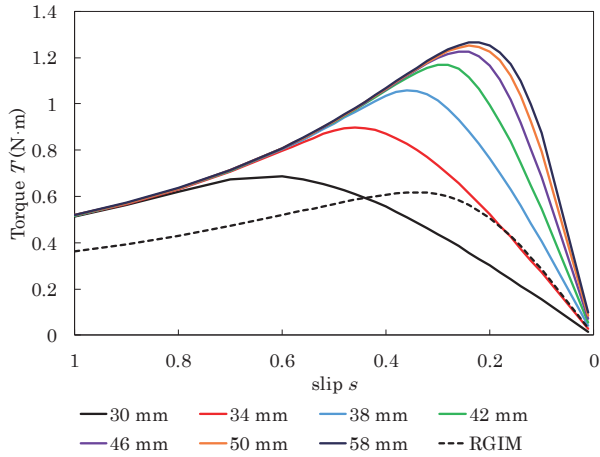


Fig. 10 Magnet flux density distribution of AGIMs.

maximum torque increased and the slip at that point decreased. It is believed that the occurrence of magnetic saturation in the region where the slip was small was suppressed by the increase in the thickness of the yoke. Figure 13 shows the relationship between torque and motor thickness. The maximum torque increased as the motor thickness increased and reached a maximum at 58 mm. However, this maximum torque resulted only due to the increasing yoke thickness, and it is expected to further increase when a tooth shape is examined. The increase in the maximum torque tended to saturate. Since the volume continues to increase even if the torque stops increasing, a motor thickness whose torque density is maximum should exist. Figure 14 shows the torque density-motor thickness characteristics. The torque density peaked at a motor thickness of 38 mm and decreased as the motor thickness further increased. When the thickness was 38 mm, the torque density was



**Fig. 11** How set yoke thickness was set.



**Fig. 12** Torque-slip characteristic at each motor thickness.

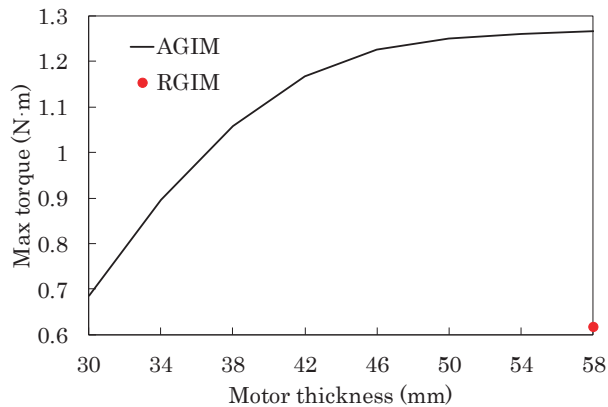


**Fig. 13** Relationship between max torque and motor thickness.

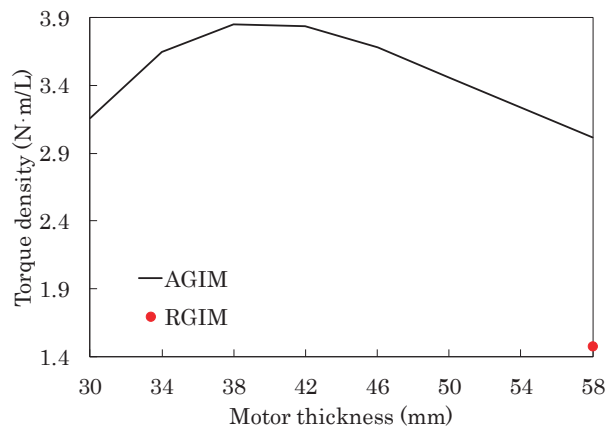


**Fig. 14** Relationship between torque density and motor thickness.

3.8 N·m/L, which was 2.62 times larger than that of the RGIM. The maximum torque was 1.06 N·m and was 1.71 times larger than that of the RGIM then. Furthermore, AGIM (38 mm) had a volume reduction of 21% from the RGIM. Thus, it was clarified that an induction motor using the toroidal winding and axial gap structure has a larger performance improvement than the conventional induction motor.

## 5. Conclusion

In this paper, an induction motor was presented that has an axial gap structure and toroidal winding, called “AGIM.” Using the proposed AGIM, the maximum torque was more than double, and the torque density was up to 2.62 times larger than that of the conventional RGIM. From these results, an advantage with respect to high torque density was demonstrated by comparing the torque density with the conventional RGIM.

In this paper, the AGIM proposed was not considered for real machine production. It is necessary to design and analyze it in consideration of real machine production in the future.

## References

- 1) H. Arihara and K. Akatsu: *ICEMS 2010*, 1681 (2010).
- 2) M. Obata, S. Morimoto, M. Sanada, and Y. Inoue: *ICEMS 2012*, DS3G2-7 (2012).
- 3) T. Nishiyama, K. Endo, and A. Matsuda: In-wheel Motor Genri to Sekkei (in Japanese), p. 128 (Kagaku Joho Syuppan, Ibaraki, 2004).
- 4) Y. Iwai, Y. Yoshida, and K. Tajima: The Papers of Technical Meeting on Magnetism, *IEE Jpn.*, MAG 15-117 (2015).
- 5) S. Aydin, T. Huang, and T. A. Lipo: *WEMPEC Research Report 2004*, 10 (2004).
- 6) Z. Nasiri-Gheidari and H. Lesani: *Przegląd Elektrotechniczny*, **88**, **2**, 300 (2012).
- 7) A. Benoudjit and N. Nait Said: *IEEE Conference*, **1**, 645 (1998).
- 8) P. L. Alger: *Induction Machines: Behavior and Uses*, p. 189 (Gordon and Breach Science Publishers, New York, 1970).
- 9) IEEJ, Denki Sekkei Gairon (in Japanese), p. 113 (Ohmsha, Tokyo, 1982).

**Received Oct. 13, 2017; Revised Dec. 10, 2017; Accepted Feb. 13, 2018**